An Anisotropic Low-Dimensional Ising System, $[(CH_3)_3NH]CoCl_3 \cdot 2H_2O$: Its Structure and Canted Antiferromagnetic Behavior

D. B. Losee,* J. N. McElearney, G. E. Shankle,† and R. L. Carlin‡
Department of Chemistry, University of Illinois at Chicago Circle, Chicago, Illinois 60680

P. J. Cresswell and Ward T. Robinson
Department of Chemistry, University of Canterbury, Christchurch 1, New Zealand
(Received 24 October 1972)

The crystal structure at room temperature and the heat-capacity and magnetic susceptibilities at low temperatures of single crystals of $[(CH_3)_3NH]CoCl_3 \cdot 2H_2O$ are reported. The orthorhombic crystals belong to the space group *Pnma* with $a = 16.671(3)$ Å, $b = 7.273(1)$ Å, $c = 8.113(2)$ Å, and $Z = 4$. The structure consists of chains of edge-sharing *trans*-$[CoCl_4(OH_2)_2]$ octahedra running parallel to the b axis. At 4.135 °K, $[(CH_3)_3NH]CoCl_3 \cdot 2H_2O$ undergoes a second-order phase transition. The heat-capacity data have been analyzed using Onsager's solution for the two-dimensional Ising model. The lattice contribution was taken into account by using the lattice of the isostructural $[(CH_3)_3NH]CuCl_3 \cdot 2H_2O$ and a corresponding states procedure. The three principal-axis single-crystal susceptibilities display an unusual amount of anisotropy. Two of the data sets (one parallel and one perpendicular to the chemical chain) have been fit to an Ising linear-chain model. A small molecular-field correction significantly improved one of those fits. The a-axis susceptibility displays an unusually sharp rise, with decreasing temperature, very close to T_N along with the suggestion of a net moment persisting below the transition. Thus, a Dzyaloshinsky–Moriya antisymmetric exchange interaction was assumed to be operative, since it is symmetry alowed in this space group, and Moriya's molecular-field-susceptibility calculation was used to fit this data set. All four of the data sets are quite reasonably described, the specific heat and one of the susceptibility sets within experimental error, by the following set of parameters: rectangular lattice exchange parameters of $J/k = (7.7 \pm 0.2)$ °K and $J'/k = (0.09 \pm 0.01)$ °K; spectroscopic splitting parameters of $g_a = 2.95 \pm 0.05$, $g_b = 3.90 \pm 0.01$, and $g_c = 6.54 \pm 0.01$; and a Dzyaloshinsky–Moriya antisymmetric exchange parameter of $|D/k| = (4.9 \pm 0.2)$ °K. Finally, a consistent spin structure is proposed in which the intrachain interaction is ferromagnetic with the compound ordering antiferromagnetically below 4.135 °K such that there is a small net moment in the a direction.

I. INTRODUCTION

The magnetic behavior of low-dimensional spin systems has recently come under intensive study. In most cases, the theoretical models describing such systems have been solved only for spin-$\frac{1}{2}$. For instance, the heat capacity of a two-dimensional Ising lattice has been reported by Onsager[1] and the parallel and perpendicular susceptibilities of isolated one-dimensional chains have also been determined.[2,3] Since Onsager's solution of the two-dimensional problem included the general case of unequal magnetic exchange for the two directions in the lattice, highly anisotropic nearly-two-dimensional compounds should be particularly interesting materials for study. Most likely, the Onsager solution could be used to describe their thermal properties while a one-dimensional model could probably still adequately explain their magnetic susceptibilities. Because Ising-like magnetic properties are often found for octahedrally coordinated Co(II), which has an effective spin of $\frac{1}{2}$ at low temperatures, chemically chained Co(II) complexes with weak links between chains are logical choices for such studies.

The crystal structure, single-crystal magnetic susceptibilities, and specific heat of just such a material, $[(CH_3)_3NH]CoCl_3 \cdot 2H_2O$, are reported in subsequent sections of this paper. The specific heat of this new compound indicates that it behaves magnetically as an anisotropic nearly-two-dimensional spin system. At the same time, definite one-dimensional properties are revealed in the susceptibilities measured along two of the crystallographic axes, while a novel form of magnetic behavior is inferred from measurements taken along the third axis. Finally, from these results a consistent spin structure for this compound is proposed.

II. CRYSTAL STRUCTURE AND PREPARATION

Trimethylammonium catena-di-μ-chlorodiaquocobalt (II) chloride, $[(CH_3)_3NH]CoCl_3 \cdot 2H_2O$, crystallizes in the orthorhombic system, space group *Pnma* (confirmed by this structure analysis) with $a = 16.671(3)$ Å, $b = 7.273(1)$ Å, and $c = 8.113(2)$ Å ($T = 24$ °C, $\lambda_{MoK\alpha_1} = 0.7093$ Å), $V = 986$ Å^3, $D_m = 1.77 \pm 0.01$ g cm^{-3} (range found in a calibrated density gradient tube) $Z = 4$, $D_x = 1.77$ g cm^{-3}.

The single crystals of $[(CH_3)_3NH]CoCl_3 \cdot 2H_2O$ used in this study were obtained by evaporating an aqueous solution containing equimolar amounts

TABLE I. (A) Fractional atomic coordinates in $[(CH_3)_3NH]\ CoCl_3 \cdot 2H_2O$. (B) Anisotropic thermal parameters. (Parameters in these tables are shown with their estimated standard errors.)

(A)

	X	*Y*	*Z*
Co	0	0	0
Cl_1	−0.09902(7)	0.25	0.00393(16)
Cl_2	0.09807(7)	0.25	−0.06583(18)
Cl_3	−0.08748(9)	0.25	0.49815(16)
C_1	0.1672(4)	0.25	0.4858(8)
C_2	0.2266(3)	0.0803(6)	0.2530(6)
N	0.1825(3)	0.25	0.3068(6)
O	0.0227(2)	0.0373(4)	0.2496(3)
H_{02}	−0.013(3)	0.106(9)	0.305(8)
H_{01}	0.461(3)	0.072(8)	0.795(7)
H_{11}	0.222(4)	0.25	0.536(7)
H_{12}	0.134(3)	0.136(7)	0.513(5)
H_{21}	0.222(3)	0.063(8)	0.128(8)
H_{22}	0.309(3)	0.019(6)	0.771(6)
H_{23}	0.282(3)	0.058(8)	0.303(7)
H_N	0.153	0.25	0.246

(B)

	B_{11}	B_{22}	B_{33}	B_{12}	B_{13}	B_{23}
Co	0.00094(3)	0.00260(15)	0.00253(12)	0.00017(4)	−0.00017(4)	−0.00036(9)
Cl_1	0.00177(5)	0.00805(23)	0.00895(21)	0	0.00021(7)	0
Cl_2	0.00191(4)	0.00876(21)	0.00825(21)	0	0.00021(8)	0
Cl_3	0.00283(5)	0.01085(26)	0.00721(21)	0	0.00024(8)	0
C_1	0.0033(3)	0.0151(14)	0.0082(10)	0	0.0001(4)	0
C_2	0.0027(2)	0.0122(8)	0.0134(8)	0.0006(3)	−0.0004(3)	−0.0034(7)
H	0.0019(2)	0.0107(9)	0.0078(7)	0	−0.0009(3)	0
O	0.0028(1)	0.0098(5)	0.0065(4)	0.0009(2)	0.0000(2)	−0.0003(4)

of $[(CH_3)_3NH]Cl$ and $CoCl_2 \cdot 6H_2O$. They are relatively stable and chemical analysis verified the empirical formula given. The crystals grow as prisms elongated along the *b* axis, usually bounded by {201} and {100} and terminated by {011}. A pronounced optical dichroism is observed in the crystals when viewed along the *a* axis with polarized light, so that with the electric vector approximately parallel to the *c* axis the crystals are blue colored. Viewed in any other direction under polarized light the crystals remain violet/red. Both the room-temperature and low-temperature optical absorption spectra of these crystals are strongly polarized.

TABLE II. Selected bond lengths and selected angles.

Selected bond lengths (Å)	
Co–O	2.078(3)
$Co–Cl_1$	2.4561(8)
$Co–Cl_2$	2.5029(8)
$Co–Cl_3$	4.665(1)
$Cl_3–H_{01}$	2.27(6)
$Cl_3–H_{02}$	2.25(7)
Co...Co	3.6366(7) along the chain.

Selected angles (deg)		
$Co–Cl_1–Co$	95.52(4)	
$Co–Cl_2–Co$	93.14(4)	
$Cl_1–Co–Cl_2$	84.49(3)	internal angle
	95.51(3)	external angle
$O–Co–Cl_1$	90.77(9)	and 89.23(9)
$O–Co–Cl_2$	89.66(9)	and 90.34(9)
$H_{01}–O–Co$	109	
$H_{02}–O–Co$	116	
$H_{01}–O–Co$	119	
$O–H_{01}–Cl_3$	153	
$O–H_{02}–Cl_3$	166	

A total of 1311 reflections, whose intensities exceeded their own estimated standard deviations, were collected using a Hilger and Watts four-circle automatic diffractometer and zirconium filtered Mo$K\alpha$ x radiation. These data were collected for two members of the form $\{hkl\}$, corrected for absorption and averaged. The structure was solved by normal methods and refined by full-matrix least-squares procedures until the conventional *R* factor was 5%. Every hydrogen atom was clearly resolved in difference Fourier synthesis.

Cobalt atoms lie on crystallographic centers of symmetry [special position (a)] and are coordinated octahedrally to four chlorine atoms and two water molecules. Although the point group of the coordination center is strictly C_i, it is quite close

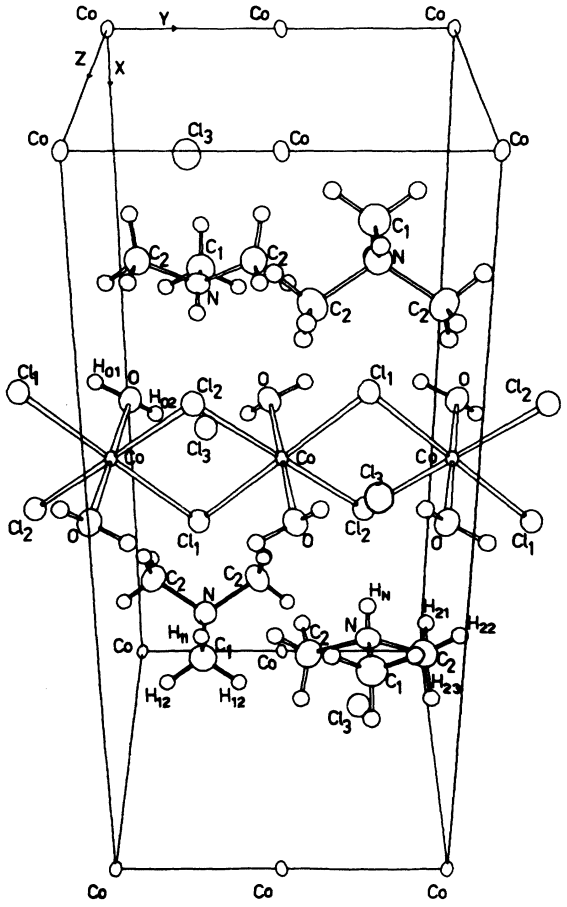

FIG. 1. Three-dimensional representation of the unit cell of $[(CH_3)_3NH]CoCl_3 \cdot 2H_2O$. For clarity, atoms bonded to the Co atoms on the edges of cell are not shown.

to D_{4h}. The octahedra share edges to form infinite chains parallel to the crystallographic b (y) direction. The fractional coordinates, anisotropic thermal parameters, and some selected bond distances are presented in Tables I and II. A three-dimensional representation of a unit cell is shown in Fig. 1, where only one of the chains is shown for clarity.

The cobalt atoms are 3.637 Å apart and linked by bridging chlorine atoms designated Cl_1 and Cl_2. The trimethylammonium cations and the remaining anionic chloride ions are found as interstitial ions with Cl_3, N, and C_1 all on the mirror planes [special position (c)] as are Cl_1, Cl_2 and two of the hydrogen atoms.

In Fig. 2 the unit cell is projected onto the ac plane and in Fig. 3 the bc plane projection of a layer section of the structure (taken parallel to the bc plane) is given. From these projections it is obvious that each $[CoCl_4(OH_2)_2]$ molecular unit is tilted with respect to adjacent units. The dihedral angle between adjacent $CoCl_4$ planes is 15.58(6)°, with the Cl_1-Cl_2 vector approximately parallel to the crystallographic a (x) axis. This angle of tilt is in the same sense for corresponding pairs of octahedra in nearest-neighbor chains (chains adjacent along [001]), while it is in the opposite sense in next-nearest-neighbor chains (chains adjacent along [101]). The layer nature of this compound is emphasized by the projection shown in Fig. 3, since the trimethylammonium cations clearly lie outside the layer used for that projection. In addition, there is clear evidence that hydrogen bonds cross-link the polymeric chains

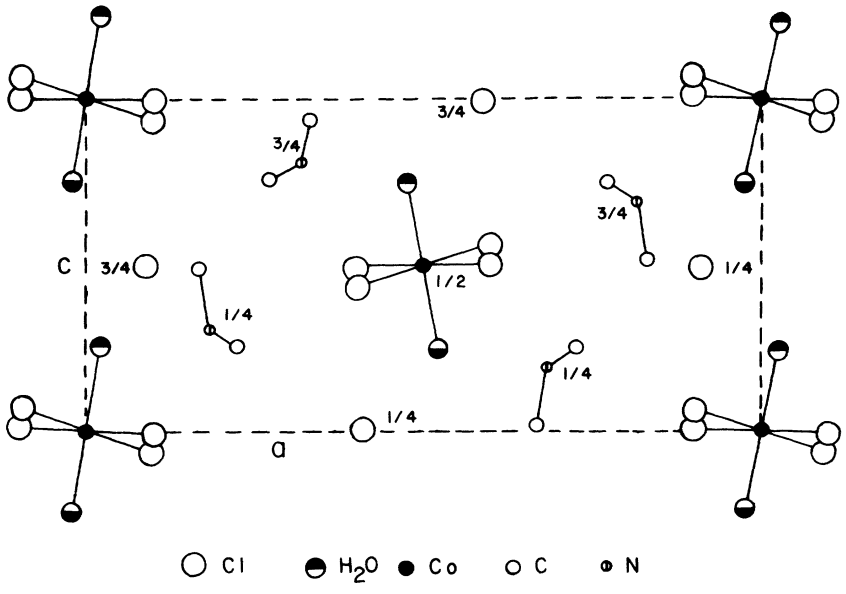

FIG. 2. Projection of the unit cell of $[(CH_3)_3NH]CoCl_3 \cdot 2H_2O$ onto the ac plane. The height above this plane of several of the atoms is indicated. (All cobalt atoms are at the same height.)

in the crystallographic c (z) direction. The anionic chlorine atom is located 1.02 Å above the center of an approximately square planar arrangement of hydrogen atoms with unique interatomic distances $Cl_3 - H_{01} = 2.59(5)$ Å and $Cl_3 - H_{02} = 2.28(7)$ Å. Thus this analysis has revealed the detailed mode of coordination of the water molecules to the cobalt ions through lone pairs of electrons with the hydrogen atoms arranged tetrahedrally with respect to these bonds. Further evidence that there are hydrogen bonds linking the chains is provided by the fact that the bc plane is a cleavage plane.

III. EXPERIMENTAL

Heat-capacity measurements on one single crystal weighing 0.7969 g were made in zero field using techniques appropriate to adiabatic calorimetry. Temperatures were measured using a calibrated germanium resistance thermometer in a dc po-

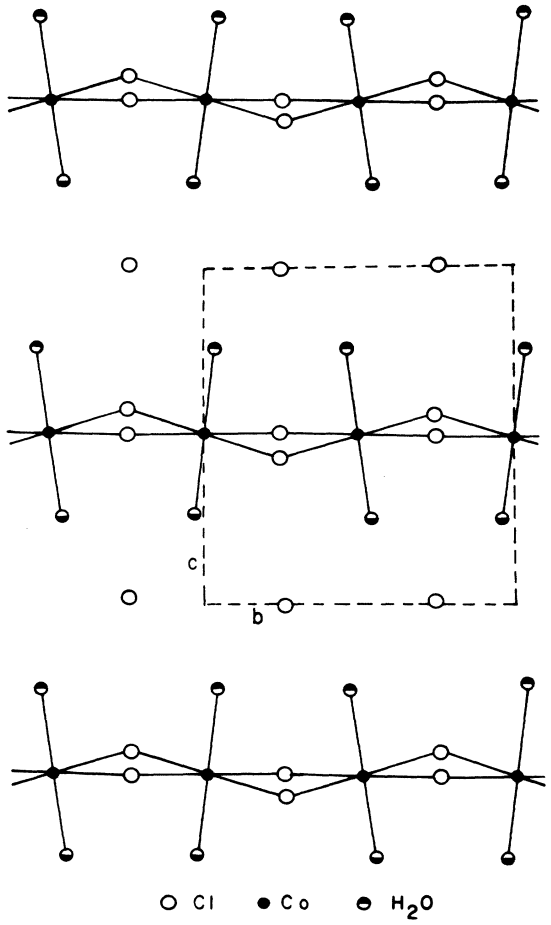

FIG. 3. Projection of a portion of the crystal structure of $[(CH_3)_3NH]CoCl_3 \cdot 2H_2O$ onto the bc plane. The portion used was a 3.33 Å thick layer taken parallel to the bc plane and centered about the cobalt atoms. The dashed lines give the unit cell boundaries.

tentiometric circuit. Two runs were made, one from 4 to 32 °K and the other from 2.75 to 32 °K. The results of these measurements are shown in Figs. 4 and 5. In the temperature regions where the two runs overlapped the reproducibility was better than 3%.

Magnetic susceptibilities were measured from 1.5 to 20 °K using a Cryotronics 17-Hz mutual-inductance bridge and a Janis variable-temperature stainless-steel Dewar. The measuring field has been estimated to be less than 15 Oe. The procedures and techniques have been described elsewhere.[4] The experimentally determined susceptibilities measured parallel to the a, b, and c axes are shown over the entire temperature region in Figs. 6 and 7. An expanded plot of their behavior below 5 °K is given in Fig. 8.

Particular attention should be paid to the widely different scales used to plot the data. Since the range of the molar susceptibilities measured between 1.5 and 20 °K covers more than three orders of magnitude, several crystals of different size had to be used for the measurements. The crystal used for the b axis measurements weighed 0.127 g and data taken with it had a measurement uncertainty of ± 0.004 emu/mole. This crystal was thoroughly dried immediately upon its removal from solution and examined with a polarizing microscope to ensure the lack of defects and pockets of occluded solution before careful orientation for measurements. The effects of misorientation or of imperfect crystallization in other samples is shown in Fig. 9 along with the results given in Fig. 6. It is apparent that the small spike occurring in those data may still be the result of a very slight misorientation or of slightly imperfect crystallization.

The measurement uncertainty for the data taken on the crystals used below 2.5 °K and above 10 °K in the a and c axes measurements is slightly larger, ± 0.005 emu/mole. The crystal used to obtain measurements of χ_c between 2.5 and 10 °K weighed 0.23 mg. Because of the smallness of this crystal, measurements made on it have an uncertainty of ± 2 emu/mole. When the same crystal was used to measure χ_a, nearly constant behavior between 2.5 and 4.3 °K was noted, with an abrupt decrease on either side. When χ_a was measured using a crystal about 30 times larger, with a correspondingly smaller uncertainty in the measurements, somewhat similar behavior was noted, with the sharp variation on the low temperature side occurring at a higher temperature; however, no numerical measurements could be taken from 3.0 to 4.3 °K, since in this region the susceptibility of this larger crystal was beyond the range of the bridge. Since the a axis of each crystal was easily identified and oriented by use of well developed (100)

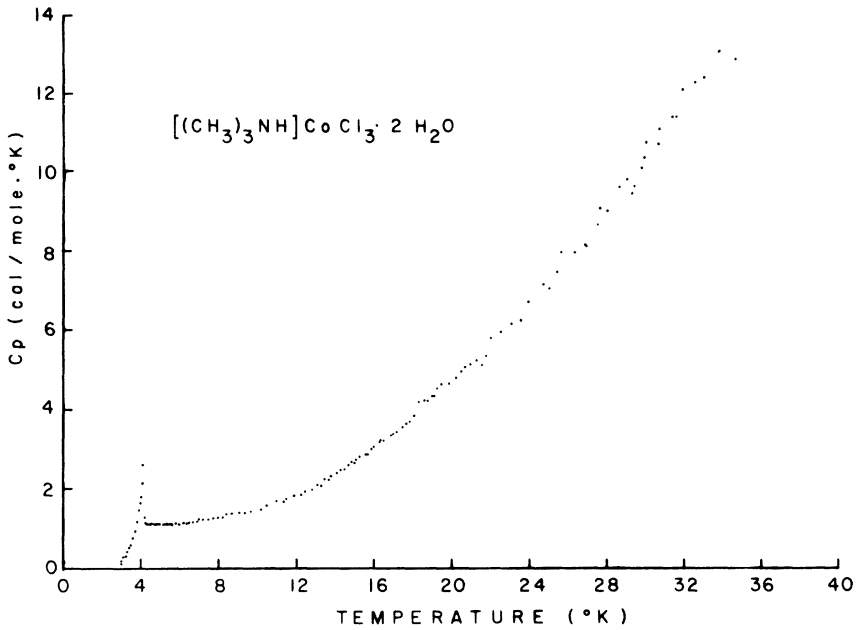

FIG. 4. Zero-field heat capacity data for $[(CH_3)_3NH]CoCl_3 \cdot 2H_2O$ between 3 and 36 °K.

faces, the likelihood that the differences in the measurements are due to misorientation is negligible.

Although demagnetization effects may be large for the orientations which exhibit large susceptibilities, no attempt has been made to correct the data due to the irregular shapes of the crystals used.

IV. RESULTS

A. Specific Heat

The experimentally determined heat capacity shows a sharp λ-type transition at (4.135 ± 0.006) °K with a nearly linear dependence on temperature from slightly above this temperature to approximately 10 °K. Below the transition temperature

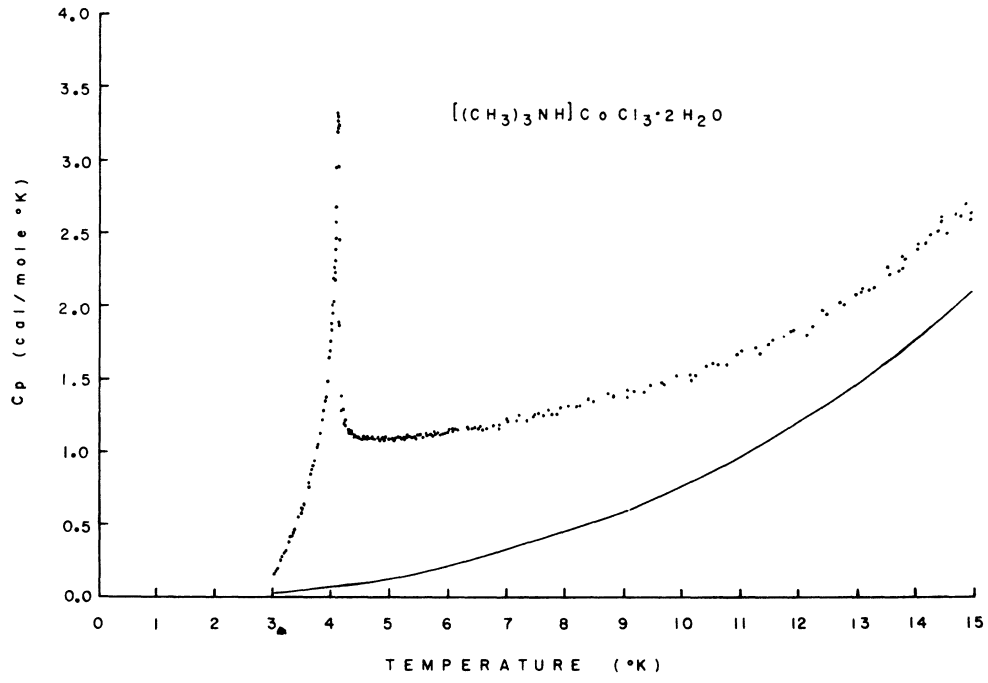

FIG. 5. Detailed representation of the heat capacity data for $[(CH_3)_3NH]CoCl_3 \cdot 2H_2O$ between 3 and 15 °K. The solid line represents the lattice contribution.

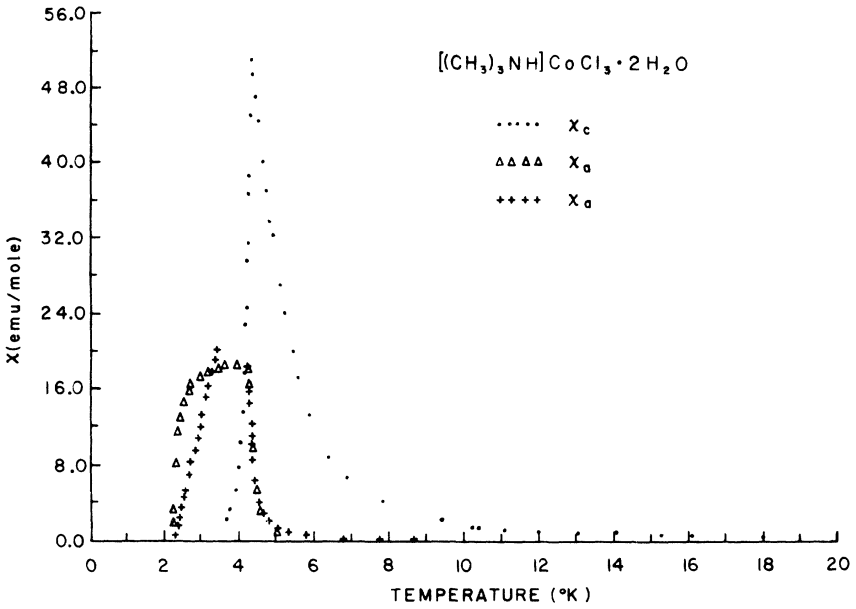

FIG. 6. Zero-field magnetic susceptibilities of $[(CH_3)_3NH]\,CoCl_3 \cdot 2H_2O$ measured along the *a* and *c* axes. The results of measurements along the *a* axis on two different crystals are shown.

there is a dramatic decrease in the measured heat capacity.

In evaluating specific-heat data it is first necessary to account for the lattice contribution. An analysis of the high-temperature data for $[(CH_3)_3NH]CoCl_3 \cdot 2H_2O$ shows that the lattice contribution does not follow a simple T^3 law as is often assumed for lattice heat capacities. In fact, the data indicate that the lattice more nearly follows a T^2 law. Therefore, in order to obtain the lattice contribution, a corresponding states approach requiring the use of the heat capacity of a diamagnetic material isomorphous to $[(CH_3)_3NH]CoCl_3 \cdot 2H_2O$ has been used.

Since such a material does not seem to exist, the isostructural, although not isomorphous, material $[(CH_3)_3NH]CuCl_3 \cdot 2H_2O$ has been used instead. Since the masses of copper and cobalt are quite similar while the remainder of each molecule is identical, the assumption of comparable vibrational contributions from both compounds to the entropy and to the heat capacity should be valid. The heat capacity of $[(CH_3)_3NH]CuCl_3 \cdot 2H_2O$ has been reported[5] from 1 to 32 °K. Above 5 °K, the magnetic effects in this material are negligible and the smoothed heat capacity data above this temperature were used directly in the following calculations. However, since the heat capacity

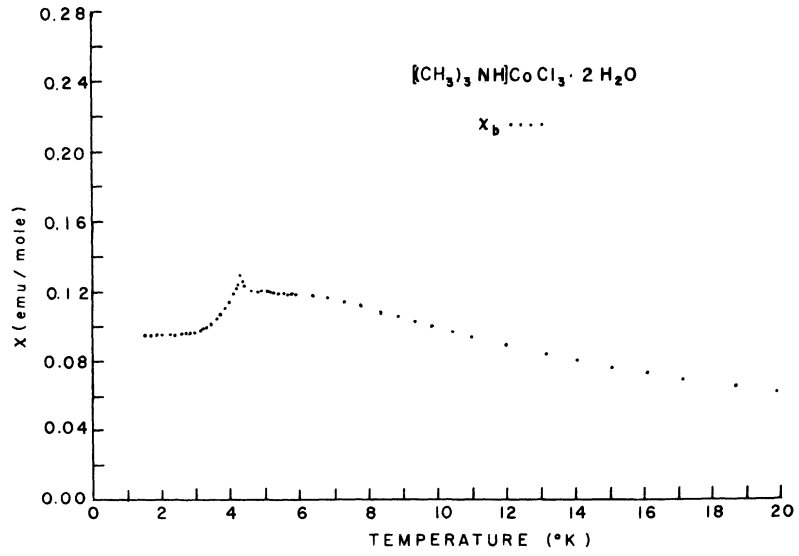

FIG. 7. Zero-field magnetic susceptibility of $[(CH_3)_3NH]CoCl_3 \cdot 2H_2O$ measured parallel to the *b* axis.

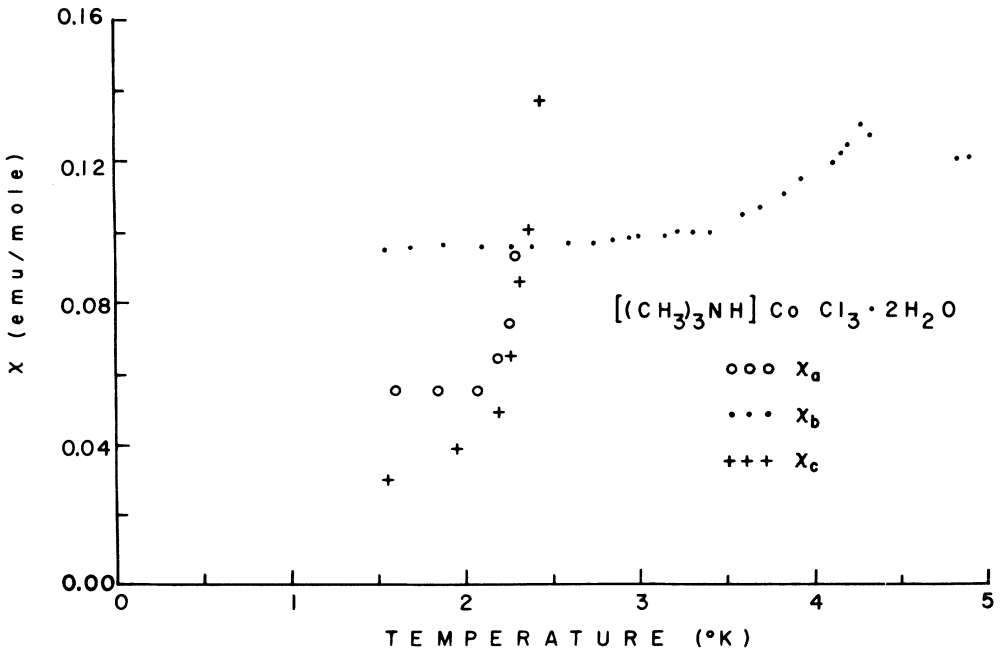

FIG. 8. Magnetic susceptibilities measured parallel to the three crystallographic axes of $[(CH_3)_3NH]CoCl_3 \cdot 2H_2O$ at low temperatures. The steep rise of χ_a (O) and χ_c (+) near 2.3 °K is evident. Additionally, although no data points were taken, χ_a was observed to be constant between 1.5 and 2 °K. Within the measurement uncertainty, χ_b (•) is also constant in that region, while χ_c definitely is not.

begins to increase below 2 °K, indicating some magnetic contributions to the measured heat capacity, the heat capacity below 5 °K of the "diamagnetic isomorph" must be obtained by subtracting from the total heat capacity the magnetic portion determined[5] from a fit of the data. These data thus furnish the specific heat of a nonmagnetic lattice which is isostructural to that of $[(CH_3)_3NH]CoCl_3 \cdot 2H_2O$.

Following Stout and Catalano's corresponding-states approach,[6] the entropy gain as a function of temperature for each compound has been used to obtain the lattice contribution to the heat capacity of $[(CH_3)_3NH]CoCl_3 \cdot 2H_2O$. The procedure assumes

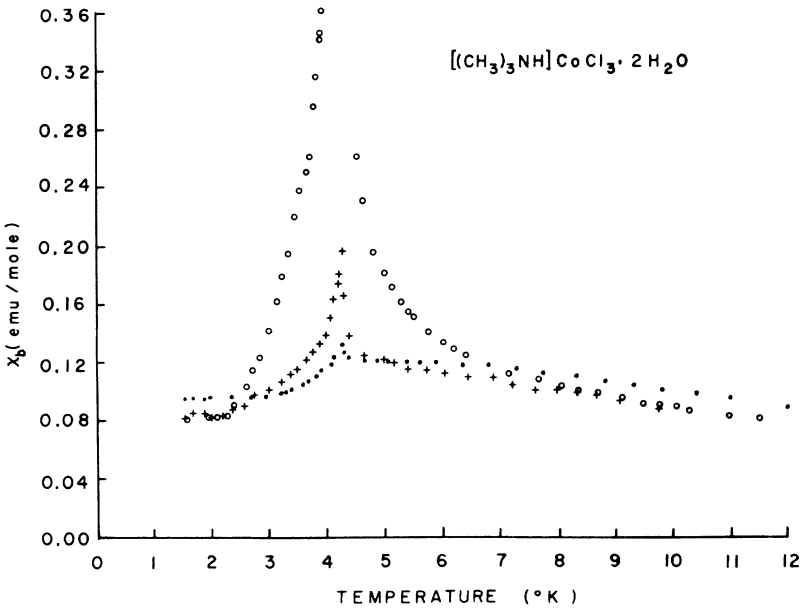

FIG. 9. Magnetic susceptibilities of three different crystals of $[(CH_3)_3NH]CoCl_3 \cdot 2H_2O$ measured parallel to the b axis. The three data sets illustrate the effect of slight misorientation or of imperfect crystallization.

that the lattice entropy gain S of isomorphous materials may be expressed by a common function ϕ, whose argument is the reduced temperature T/θ, where θ is compound dependent. For two compounds, 1 and 2, at corresponding temperatures T_1 and T_2, it follows that if $S_1 = S_2$, then $\phi(T_1/\theta_1) = \phi(T_2/\theta_2)$ and therefore $T_1/\theta_1 = T_2/\theta_2$ or $T_1/T_2 = \theta_1/\theta_2$. This latter ratio is denoted as the corresponding states ratio r. If the corresponding states assumption is valid, r must be a constant. In practice, r generally is not constant but rather has a slight temperature dependence. If there is a magnetic contribution to the total measured entropy for one of the materials being compared, this contribution must be subtracted from that entropy before the corresponding states argument may be applied and the resulting entropy used to obtain the value of r relating the two compounds. Since that contribution is generally unknown and changing with temperature, the total expected magnetic entropy contribution must be subtracted instead. As this will be an overestimate throughout the region where there is a magnetic contribution to the entropy, only becoming valid above that region, it is to be expected that the r resulting from a corresponding states calculation in that region will not be constant. As the contribution to the magnetic entropy approaches the total expected value, the value of r will exhibit the near-constant behavior expected. The nonmagnetic heat capacity determined for $[(CH_3)_3NH]CuCl_3 \cdot 2H_2O$, C_{Cu}, and the measured heat capacity of the cobalt compound have been used, respectively, in the above corresponding states procedure to determine r as a function of temperature. The results are shown in Fig. 10 and the expected near-constant behavior of r is seen to begin above about 18 °K. In order to obtain valid values of r below that temperature, r was assumed to be a linear function of temperature, $r = a + bT$. A least-squares fit of the data above about 18 °K resulted in values of $a = 1.042$ and $b = -5.54 \times 10^{-4}$. The lattice contribution to the heat capacity of the cobalt compound may then be obtained from

$$C_{lat}(T) = T\frac{dS_{lat}(T)}{dT}$$

$$= T\frac{dS_{Cu}(rT)}{d(rT)}\,\frac{d(rT)}{dT}$$

$$= C_{Cu}(rT)\,(a + 2bT)/(a + bT)\,. \qquad (1)$$

The corresponding-states lattice heat capacity for $[(CH_3)_3NH]CoCl_3 \cdot 2H_2O$, shown as the smooth line in Fig. 5, was thus subtracted from the measured heat capacity giving the magnetic contribution shown as a smooth line in Fig. 11. Taking into account the accuracy of the data used to calculate r and the uncertainty in the extrapolation of r, it is estimated that the resulting magnetic contribution to the heat capacity of $[(CH_3)_3NH]CoCl_3 \cdot 2H_2O$ is known to within 7%. Since by 20 °K the magnetic contribution has dropped to only 5% of the net measured specific heat, little quantitative significance can be attached to the data above this temperature.

As can be seen in Fig. 12, where the integral $S = \int_0^T (C_{mag}/T')dT'$ has been evaluated, only 8% of the theoretical maximum entropy for a mole

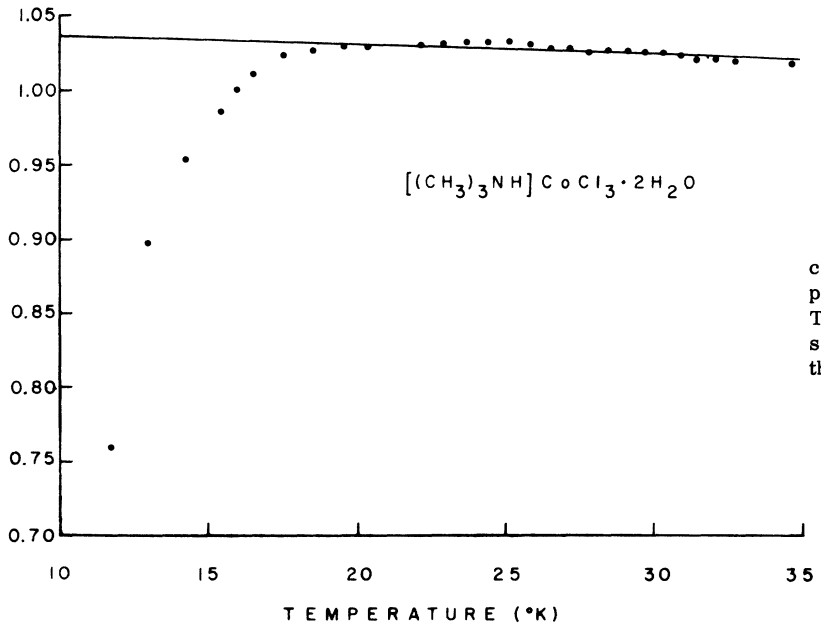

FIG. 10. Experimentally determined corresponding states ratio r vs temperature for $[(CH_3)_3NH]CoCl_3 \cdot 2H_2O$. The solid line represents the best straight-line extrapolation used for the lattice determination.

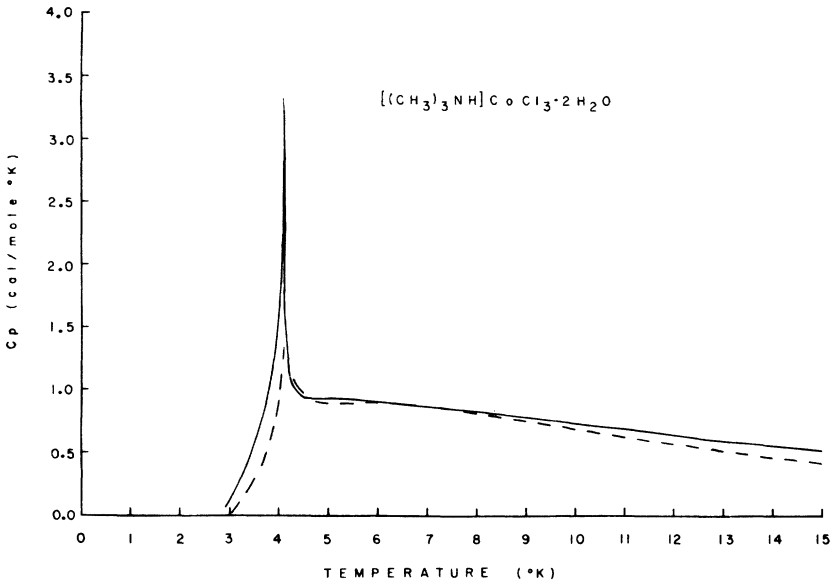

FIG. 11. Magnetic heat capacity (solid line) of $[(CH_3)_3NH]CoCl_3 \cdot 2H_2O$ from 3 to 15 °K. The dashed line represents the fit to Onsager's equation as described in the text.

of spin-$\frac{1}{2}$ Co^{2+} ions, $R\ln 2$, has been acquired at the transition temperature. By 20 °K, 96% of this maximum entropy has been acquired. Thus substantial short range order persists from 4.135 °K to well above 15 °K in this compound. This short-range order is an indication of the lowered dimensionality of the magnetic spin system.

Since the crystal structure analysis clearly shows the compound to consist of sheets of cross-linked infinite chains, the magnetic heat capacity for $[(CH_3)_3NH]CoCl_3 \cdot 2H_2O$ has been fit to Onsager's solution[1] for the heat capacity of an anisotropic two-dimensional (anti-) ferromagnet. Onsager's expression for the partition function of the two-dimensional lattice is

$$z = [2.0 \sinh(2H)]^{1/2} \exp\{[\int_0^{\pi} \alpha(\omega) d\omega]/2\pi\}^{1/2}, \tag{2}$$

where

$$\cosh[\alpha(\omega)] = [\cosh(2H')/\tanh(2H)] - [\sinh(2H')/\sinh(2H)]\cos\omega, \tag{3}$$

with $H = J/kT$ and $H' = J'/kT$, and where J and J' are the nearest-neighbor exchange parameters of the rectangular lattice. Since the heat capacity is related to the partition function by

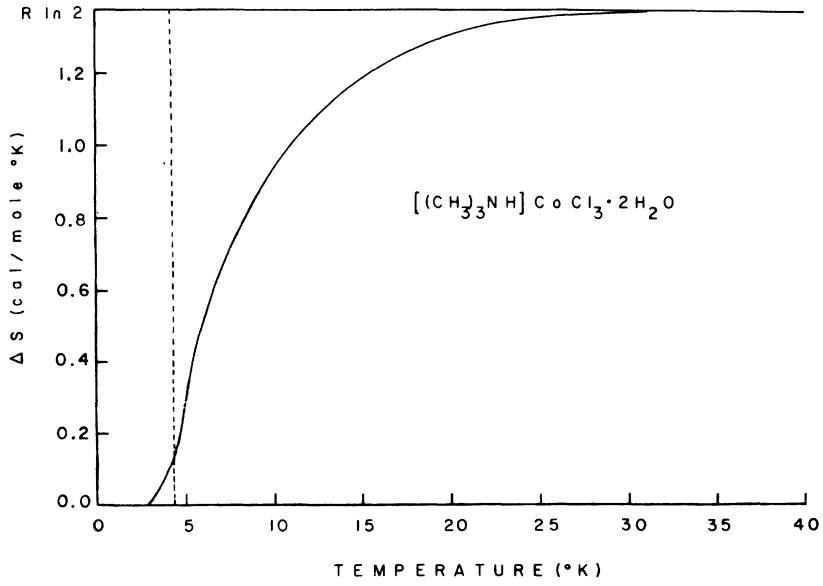

FIG. 12. Magnetic entropy of $[(CH_3)_3NH]CoCl_3 \cdot 2H_2O$ as a function of temperature. The dashed line indicates the ordering temperature.

$$C_p = \frac{\partial}{\partial T}\left(NkT^2\,\frac{\partial(\ln z)}{\partial T}\right), \tag{4}$$

the heat capacity for a rectangular lattice is easily calculated numerically. Heat capacities thus calculated were fit to the experimentally determined values using a least-squares procedure. All calculations were performed in double precision on the U. I. C. C. IBM 370/155.

A temperature region from 4.2 to 15 °K was used to fit the data. The values resulting from this fit are $|J/k| = (7.7 \pm 0.2)$ °K and $|J'/k| = (0.09 \pm 0.01)$ °K. The transition temperature T_N these parameters predict may be calculated by a numerical solution of the equation

$$\sinh(2J/kT_N)\sinh(2J'/kT_N) = 1. \tag{5}$$

Although the value thus calculated, 4.05 °K, is slightly lower than that observed experimentally, 4.135 °K, the agreement is quite satisfactory. The fitted specific heat is shown in Fig. 11 as a dashed line and although it is consistently low over most of the fitted region, it is within the error bounds except at the very highest temperature. It should be noted that at the transition the experimental specific heat does not rise above 3.4 cal/mole °K, although the theory predicts it should become infinite at that temperature. Furthermore, below the transition the calculated curve decreases with decreasing temperature even more quickly than observed experimentally.

A possible explanation for these observed differences is the presence of additional, smaller exchange interactions. Because the ratio of J' to J is approximately 1 to 100, it is not unreasonable to assume that in the temperature region above the transition, where there is only short-range order, these extra interactions will have little effect. However, they should be expected to have more of an effect below the transition where they undoubtedly influence the long-range order.

B. Susceptibility

Although Co(II) in an octahedral environment usually exhibits magnetic anisotropy, the single crystal magnetic susceptibilities of $[(CH_3)_3NH]CoCl_3 \cdot 2H_2O$ show an exceptional anisotropy, with dramatically different behavior of each principal axis susceptibility. At 4.33 °K the susceptibility measured along the chemical chain is approximately $\frac{1}{500}$ of that measured perpendicular to the chain along the c axis. Slightly below this temperature the principal axis susceptibilities undergo abrupt changes. In addition, the easy and hard axes are switched at the two extremes of the temperature region investigated.

If the transition temperature is defined from the susceptibility data as the point of maximum positive slope, a value of $T_N = (4.30 \pm 0.03)$ °K is obtained from the c axis data. The difference between this value and that obtained from the heat capacity measurements (4.135 ± 0.006) °K, may be due to the field of the measuring coil. Below about 3 °K much of the anisotropy disappears. As shown in Fig. 8, χ_a and χ_b remain constant with decreasing temperature, while χ_c tends to zero. At least in the lowest temperature region, the susceptibility behavior appears similar to that of an antiferromagnet in the ordered state, with χ_c behaving as $\chi_\parallel$ and χ_a and χ_b as $\chi_\perp$.

However, it is obvious upon consideration of the measured magnitudes of χ_a and χ_c at higher temperatures that the transition occurring in this compound is not a simple paramagnetic to antiferromagnetic one. This is further confirmed when the Curie–Weiss equation, $\chi = Ng^2\mu_B^2 S(S+1)/[3k(T-\theta)]$, is used to fit the data in the temperature region from 15 to 20 °K. In this restricted temperature region each data set was fitted within the stated experimental errors. The resulting values for the parameters from the fits are listed in Table III. The Curie–Weiss-determined g values tabulated in Table III add to 14.45, which is approximately 10% above 13, the value to which the g values associated with the ground doublet of Co^{2+} in an octahedral environment should sum.[7] Atypical magnetic behavior is indicated by the signs of the various θ's. The θ's of the large susceptibility directions have positive values, while the small direction has the negative θ usually associated with antiferromagnetic exchange. This unusual behavior is a reflection of the usual anisotropy of Co(II) combined with the anisotropy of the crystal lattice.

Since the problem of calculating the susceptibility of an anisotropic two-dimensional magnetic system has not been solved yet, and since the heat capacity results have indicated the exchange between the cross-linked chains in $[(CH_3)_3NH]CoCl_3 \cdot 2H_2O$ to be relatively small, the susceptibility results have been fitted using equations based upon isolated, noninteracting Ising linear chains. The Hamiltonian[2,3] for a one dimensional Ising system with a magnetic field in the xz plane may be written

$$\mathcal{H} = -J\sum_{i,j}\sigma_i^z\sigma_j^z - g_z H_z\sum_i \sigma_i^z - g_x\mu_B H_x\sum_i \sigma_i^x\,. \tag{6}$$

TABLE III. Curie–Weiss fit in high-temperature region for $[(CH_3)_3NH]CoCl_3 \cdot 2H_2O$.

	g	θ(°K)
χ_a	3.31 ± 0.05	1.32 ± 0.05
χ_b	3.59 ± 0.05	-1.06 ± 0.05
χ_c	7.55 ± 0.08	7.75 ± 0.09

Two cases must be considered. The Hamiltonian resulting for $H_x = 0$ gives rise to the susceptibility[3]

$$\chi_z = (Ng^2\mu_B^2/4kT)e^{2J/kT} . \quad (7)$$

For $H_z = 0$, the susceptibility calculated from Eq. (6) is[2,3]

$$\chi_x = (Ng^2\mu_B^2/8|J|)[\tanh(|J|/kT) + (|J|/kT)\operatorname{sech}^2(|J|/kT)]. \quad (8)$$

Generally, when theoretical fits are attempted on single crystal linear chain susceptibility data, both of the above equations must be considered, regardless of the direction of measurement of the data. Note that the z axis, that is, the anisotropy axis, may be determined if fits of mutually orthogonally measured data sets can be obtained by consistent use of Eqs. (7) and (8).

When Eq. (7) was used to fit the susceptibility measured parallel to the chemical chain, χ_b, a fit within the stated error bounds from 6 to 20 °K resulted with values of $J/k = (2.22 \pm 0.01)$ °K and $g = 4.08 \pm 0.01$. However, an equally good fit of the same data was achieved with Eq. (8) by using $|J/k| = 7.7$ °K, the value determined from the heat capacity data, and a g value of 3.90 ± 0.01. It is particularly satisfying in the latter case to achieve an excellent fit with an exchange constant from an independent measurement. However, what is even more gratifying is the observation that the exchange constant and g value also predict within experimental error the behavior of χ_b below the transition. This fit is shown over the entire temperature region in Fig. 13. On the other hand, the fitted values from Eq. (7) give neither quantitative nor qualitative agreement with the experimental values below the transition.

Similarly, for susceptibilities measured along c, a direction obviously perpendicular to the chemical chain, it is found that only Eq. (7) with a positive exchange constant generates values as large as

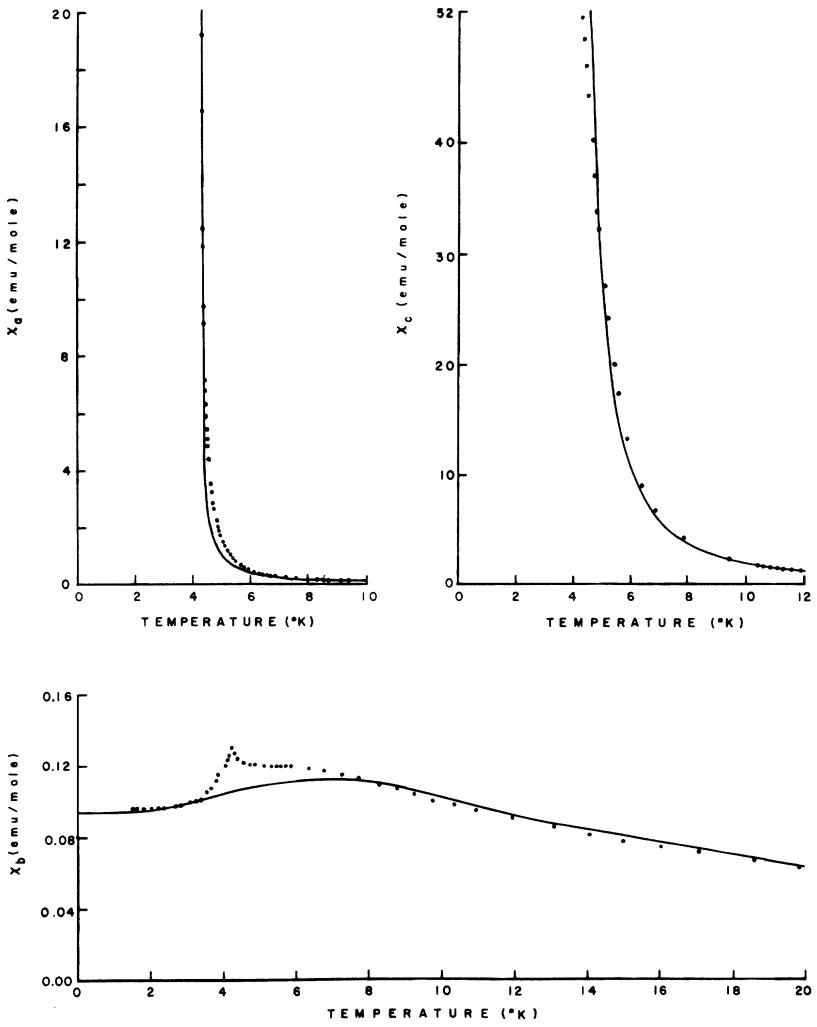

FIG. 13. Results of the best-fit analyses (solid lines) of the three principal axis magnetic susceptibilities as described in the text.

the observed susceptibility. Again, setting J/k equal to the value from the heat capacity, 7.7 °K, and varying g, qualitatively correct behavior from 4.3 to 20 °K is achieved with $g = 6.54 \pm 0.01$. The fit is considerably improved close to the transition by including the effects of a molecular exchange field[8,9] along the c axis, J':

$$\chi_c = \frac{\chi_s}{1 - (2zJ'/Ng^2\mu_B^2)\chi_s} , \tag{9}$$

with $zJ'/k = (0.17 \pm 0.02)$ °K.

Although this fit, shown in Fig. 13, is not within the stated error bounds, the fitted values are within 12% of the measured values. This is quite good agreement when the demagnetizing effects that must be associated with these large susceptibility values are considered. Additionally, it must be noted that since the above molecular field calculation makes use of the susceptibility of linear chains the number of nearest-neighbors parameter in that calculation, z, refers to the number of nearest linear chain neighbors to a given chain. Thus, since there are two nearest-neighbor chains (along the c axis) for any given chain, $J'/k = 0.085$ °K, in gratifying agreement with the heat-capacity result of $|J'/k| = 0.09$ °K. Furthermore, the positive values of J and J' determined above indicate ferromagnetic coupling in both the b and c directions. Also note that the use of Eq. (7) implies that the spins are quantized along the c axis and that this is consistent with the susceptibility behavior at low temperatures, which implies that the c axis is the easy axis.

Although the a axis is also perpendicular to the chains in $[(CH_3)_3NH]CoCl_3 \cdot 2H_2O$, data measured along the axis cannot be fit using either Eqs. (7) or (8). A clue to the reason is given by the behavior of χ_a below 4.3 °K. The region of large, nearly constant susceptibility observed seems to indicate the presence of a net moment along the a axis. The differences between those regions in the two a-axis data sets may be interpreted as evidence of the field dependence of that net moment, since the demagnetizing factors in the two sets of measurements are probably quite different, owing to the large difference in the sizes and shapes of the samples used for the two sets of measurements, thus creating different internal fields. The good agreement of the two data sets above 4.3 °K supports this view in that obviously misalignment cannot be the cause of the differences.

Such behavior might well be expected for a canted spin system which is weakly ferromagnetic. In fact, behavior similar to that of χ_a in the paramagnetic region has been predicted by Moriya.[10] Using a Hamiltonian of the form

$$\mathcal{H} = -J \sum_{i,j} \vec{S}_i \cdot \vec{S}_j + B_j \sum_j (S_j^z)^2 + D \sum_{i,j} (S_i^x S_j^y - S_i^y S_j^x) - g\mu_B \vec{H} \cdot \sum_j \vec{S}_j \tag{10}$$

with a molecular field approximation, Moriya has predicted a very sharp change in the temperature variation of the paramagnetic susceptibility close to T_N for a canted spin system. For a spin-$\frac{1}{2}$ linear chain the susceptibility measured along the direction of the weak ferromagnetic moment should be given by[10]

$$\chi = Ng^2\mu_B^2(T - T_0)/[4k(T^2 - T_N^2)] , \tag{11}$$

where T_N and T_0 are given by

$$T_N = -(J/2k)[1 + (D/J)^2]^{1/2} , \tag{12}$$

$$T_0 = -J/2k . \tag{13}$$

To avoid the usual poor prediction of the transition temperature by molecular field approximations, T_N may be set equal to the actual transition temperature of 4.30 °K. In that case

$$T_0 = -T_N/[1 + (D/J)^2]^{1/2} . \tag{14}$$

Thus Eqs. (11) and (14) were used to fit the χ_a data. The fit, which describes quite well the behavior of χ_a from 4.3 to 20 °K, was achieved with $g_a = 2.95 \pm 0.05$ and $|D/J| = 0.64 \pm 0.02$ [for $J/k = 7.7$ °K, $|D/k|$ then is equal to (4.9 ± 0.2) °K]. Although this fit, shown in Fig. 13, is not within the stated error bounds, to expect otherwise would be unreasonable since demagnetization effects have been ignored and a molecular field approximation has been used.

The parameters determined from the three sets of susceptibility measurements are summarized in Table IV. The g values resulting from the fits of χ_a, χ_b, and χ_c sum to a value of 13.39, which is in excellent agreement with the prediction for Co^{2+} and is a considerable improvement over the Curie–Weiss sum. Furthermore, it should be noted that the anisotropy between χ_a and χ_b at low temperatures is quite well predicted by using the above g values in the low temperature limit[3] of Eq. (8):

$$\chi_x(0) = Ng^2\mu_B^2/8J . \tag{15}$$

For $J/k = 7.7$ °K and the corresponding g values, χ_a and χ_b are predicted to be 0.053 and 0.093 emu/mole, respectively. The measured values are 0.056 and 0.096 emu/mole, respectively.

V. DISCUSSION

Although the detailed spin structure of $[(CH_3)_3NH]CoCl_3 \cdot 2H_2O$ will not be known until either neutron diffraction or NMR studies are completed, it still is possible to postulate a reasonable spin arrangement for this compound which is completely consistent with the above results.

These results have revealed a highly anisotropic

TABLE IV. Zero-field magnetic susceptibility results for $[(CH_3)_3NH]CoCl_3 \cdot 2H_2O$.

	χ_a	χ_b	χ_c
Eq.	(11), (14)	(8)	(7), (9)
J/k(°K)	7.7 ± 0.2	7.7 ± 0.2	7.7 ± 0.2
$\lvert D/J \rvert$	0.64 ± 0.02	...	...
zJ'/k(°K)	...	...	0.17 ± 0.02
g	2.95 ± 0.05	3.90 ± 0.01	6.54 ± 0.01

nearly two-dimensional spin system. This system may be pictured as consisting of one-dimensional chains of spins, chained along b, which are weakly cross-linked in the c direction. The spins have essentially no b components and lie in the ac plane. The coupling along each chain is strongly ferromagnetic such that it causes spin quantization nearly along c, perpendicular to the chain direction. This coupling, taken with the crystal symmetry, requires that the c components of spins in a given chain all be equal and parallel to each other. Similarly, all of the a components of a chain's spins must be equal and parallel. The b components, if any, must be equal and antiparallel. Nearest interchain neighbor spins of nearest-neighbor chains are aligned parallel to each other. The nearest interchain neighbor spins of next-nearest-neighbor chains most likely are aligned such that their c components are equal and antiparallel, while their a components are equal and parallel. The spin structure is most easily pictured by considering that the spins are oriented in some consistent manner with respect to the O–Co–O bonds of each $[CoCl_4(OH_2)_2]$ unit. If the a components of the spins are nonzero, such a spin structure results in a weak ferromagnet, or in other words, a canted antiferromagnet, with canting and a net moment along a.

The above spin structure is not only supported by the satisfactory fits of the data achieved, but also by the presence of a net moment along a immediately below T_N. In addition, this picture is completely consistent with the crystal symmetry which allows spin canting along a and hidden spin canting along b. However, were such hidden spin canting present, χ_b would be expected to behave much more like χ_a in the region slightly above T_N. Then, below T_N, it would drop to a small value, reflecting the necessary antiferromagnetic ordering along b, rather than remain constant as χ_a does. Although there may be such behavior for a very small interval, it more likely has resulted from imperfect crystallization or misorientation. If there is any hidden canting of spins along b, the angle of the cant must be exceedingly small.

In any case, some interesting observations regarding the canting that the data clearly show should be noted. The most notable feature of the canting, as shown by the behavior of χ_a, is that the net moment along a clearly disappears at low temperatures. The disappearance is apparently gradual and its rate varies between crystals. As might be expected for such a gradual change, no obvious corresponding anomalous behavior is observed in the heat capacity data below T_N. Three plausible explanations may be given. A spin reorientation may take place such that the magnetic unit cell is increased in size in such a way that the spins remain canted without any net moment resulting. However, a heat capacity anomaly most likely would be observed in this case. Possibly, a domain structure might explain the behavior. Or possibly the spins gradually line up perfectly along c, or at least completely into the bc plane. (The low temperature data still allow a small amount of hidden canting along b.) A fourth possibility could be that the behavior is a result of an inability of the moments to respond to the ac measuring field at lower temperatures. However, the nearly constant nonzero behavior of χ_a at the lowest temperatures (which was noted to be consistent with the linear chain model used as well as with the parameters determined in the paramagnetic region) would seem to disallow this possibility. Further experiments in a magnetic field should be helpful in elucidating the situation.

Perhaps a better understanding of the disappearance of the net moment would be possible if more were known about the specific mechanisms involved in the canting in this system. Single ion anisotropy,[10] antisymmetric superexchange[10] and g value anisotropy[7,11] all have been shown to produce spin canting. Only the latter two cases are possibilities here. If antisymmetric exchange is the cause, and if the exchange interaction between next-nearest-neighbor chains were known, it would be possible to calculate the angle of cant. Unfortunately, the present data do not give the necessary information. On the other hand, if the g value anisotropy is the origin of the canting, then the approximate canting angles may be calculated if the g tensor principal axes and principal g values are known. Assuming the principal g values are essentially the same as the crystallographic g values with the largest g value axis being the O–Co–O direction, a cant angle of approximately 3° away from c towards a and less than 0.5° away from c toward b is predicted using the measured g values. Quite possibly both effects contribute to the canting, but further data are required for a detailed analysis.

The spin structure within a given chain should be compared with those of two other Co(II) compounds which have similar chemical chains which

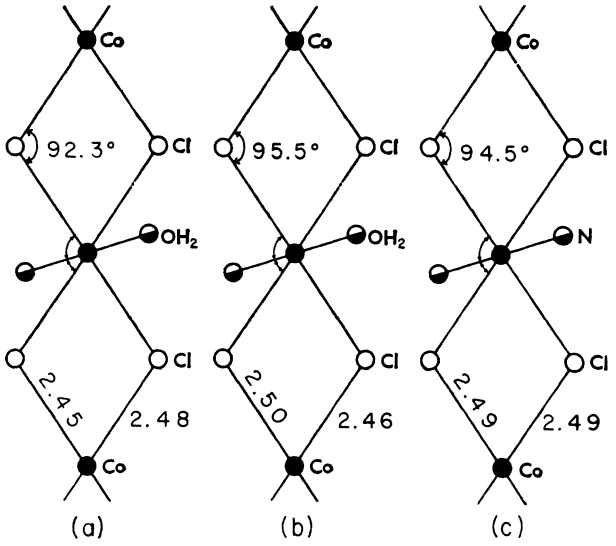

FIG. 14. Comparison of polymeric cobalt chains: (a) $CoCl_2 \cdot 2H_2O$; (b) $[(CH_3)_3NH]CoCl_3 \cdot 2H_2O$; (c) $CoCl_2 \cdot 2NC_5H_5$. All angles marked but unlabeled are approximately 90°. Bond distances are in Å.

are isolated to varying extents. The crystal structures of $CoCl_2 \cdot 2H_2O$[12] and $CoCl_2 \cdot 2NC_5H_5$,[13] like that of $[(CH_3)_3NH]CoCl_3 \cdot 2H_2O$, reveal polymeric chains of $(-CoCl_2-)$ units with either water or pyridine molecules completing the distorted octahedron. These polymeric chains are compared in Fig. 14.

While there is no spin canting allowed in $CoCl_2 \cdot 2H_2O$, this study has shown a canting between spins of next-nearest-neighbor chains producing a weak ferromagnetic moment in $[(CH_3)_3NH]CoCl_3 \cdot 2H_2O$. Although symmetry allows for spin canting in $CoCl_2 \cdot 2NC_5H_5$, such behavior is not apparent from the powder susceptibility data.[14]

It has been established by Narath[15] (from the susceptibility and NMR results) that the intrachain interaction in $CoCl_2 \cdot 2H_2O$ is ferromagnetic. The susceptibility results for $CoCl_2 \cdot 2NC_5H_5$[14] seem to indicate that the intrachain interaction in that material is also ferromagnetic, although much more convincing proof could have been established if a single crystal study had been performed. This study has shown that the intrachain interaction in $[(CH_3)_3NH]CoCl_3 \cdot 2H_2O$ is likewise ferromagnetic. At least in this series of d^7 compounds which have obvious $\approx 90°$ Co-Cl-Co exchange pathways, Anderson's superexchange theory,[16] which predicts that a 90° interaction pathway will favor ferromagnetic exchange, agrees with the experimental observations.

Although the magnitudes of the intrachain exchange for the members of this series do not appear to follow any obvious bond angle or bond distance correlation, the most trustworthy values for the exchange constants (for $CoCl_2 \cdot 2H_2O$, $J/k = 9.3\ °K$[17] and for $[(CH_3)_3NH]CoCl_3 \cdot 2H_2O$, $J/k = 7.7\ °K$) do reflect the nearest-neighbor Co-Co distances of 3.55 Å for $CoCl_2 \cdot 2H_2O$[12] and 3.64 Å for $[(CH_3)_3NH]CoCl_3 \cdot 2H_2O$. The relative isolation of chains in the two compounds is reflected in the interchain exchange. A value of 4.1 °K is reported[17] for that parameter in $CoCl_2 \cdot 2H_2O$, while it is 0.09 °K in $[(CH_3)_3NH]CoCl_3 \cdot 2H_2O$. It is likely that the corresponding exchange constant for $CoCl_2 \cdot 2NC_5H_5$ will be even smaller than that reported herein for the trimethylammonium complex. The heat capacity and susceptibility results on these compounds have essentially verified the relative isolation of these chains, as indicated by the observed transition temperatures. A transition at approximately 17 °K occurs for $CoCl_2 \cdot 2H_2O$.[18] From the present study, $[(CH_3)_3NH]CoCl_3 \cdot 2H_2O$ has been found to order at 4.135 °K, while the compound containing the most isolated linear chains, $CoCl_2 \cdot 2NC_5H_5$, orders at 3.17 °K.[14] These values, as well as the intrachain exchange in these compounds are seen to be consistent with the actual nearest interchain neighbor Co-Co distances which are 5.6 Å, 8.1 Å, and 8.7 Å, respectively.

VI. CONCLUSIONS

In conclusion, specific heat and susceptibility measurements have shown that $[(CH_3)_3NH]CoCl_3 \cdot 2H_2O$ behaves as a canted highly anisotropic, nearly two-dimensional spin system. Although this is not the first canted chain to be reported, since an antiferromagnetic arrangement of spins in a canted linear chain has been reported[19] for $CsCoCl_3 \cdot 2H_2O$, it is the first linear-chain material for which canting has been observed along with ferromagnetic intrachain exchange. The apparent low dimensionality and clear Ising-like qualities should considerably simplify theoretical interpretations of future experiments on this compound.

This fact along with the stability of the material and the ease of growing large single crystals with well-defined characteristics make $[(CH_3)_3NH]CoCl_3\ 2H_2O$ an ideal material for extensive study, especially since it is a member of an entire series of compounds which all display similar magnetic properties. The magnetic properties of the other members of this series, which has the general formula $[(CH_3)_3NH]MX_3 \cdot 2H_2O$ (where M = Mn, Ni, Co, Cu and X = Cl, Br), will be reported elsewhere.

ACKNOWLEDGMENTS

The authors wish to thank Professor J. A. Cowen for several very useful discussions. This research was supported in part by Grant No. GP-12106 of the National Science Foundation.

*Present address: Department of Chemistry, University of North Carolina, Chapel Hill, N. C. 27514.
†Present address: Department of Chemistry, Angelo State University, San Angelo, Tex. 76901.
‡Address correspondence to this author.

[1]L. Onsager, Phys. Rev. **65,** 117 (1944).
[2]S. Katsura, Phys. Rev. **127,** 1508 (1962).
[3]M. E. Fisher, J. Math. Phys. **4,** 124 (1963).
[4]J. N. McElearney, D. B. Losee, S. Merchant, and R. L. Carlin, J. Chem. Phys. **54,** 4585 (1971).
[5]D. B. Losee, J. N. McElearney, A. E. Siegel, R. L. Carlin, A. Khan, J. P. Roux, and W. J. James, Phys. Rev. B **6,** 4342 (1972).
[6]J. W. Stout and E. Catalano, J. Chem. Phys. **23,** 2013 (1955).
[7]I. F. Silvera, J. H. M. Thornley, and M. Tinkham, Phys. Rev. **136,** A695 (1964).
[8]T. Watanabe, J. Phys. Soc. Jap. **17,** 1856 (1962).
[9]J. N. McElearney, D. B. Losee, S. Merchant, R. L. Carlin, Phys. Rev. B **7,** 3314 (1973).
[10]T. Moriya, Phys. Rev. **120,** 91 (1960).
[11]E. A. Turov, *Physical Properties of Magnetically Ordered Crystals* (Academic, New York, 1965).
[12]B. Morosin and E. J. Graeber, Acta Crystallogr. **16,** 1176 (1963).
[13]J. D. Dunitz, Acta Crystallogr. **10,** 307 (1957).
[14]K. Takeda, S. Matsukawa, and T. Haseda, J. Phys. Soc. Jap. **30,** 1330 (1971).
[15]A. Narath, Phys. Rev. **136,** A766 (1964); Phys. Rev. **140,** A552 (1965).
[16]P. W. Anderson, in *Magnetism*, edited by G. T. Rado and H. Suhl (Academic, New York, 1963), Vol. 1, Chap. 2.
[17]A. Narath, Phys. Lett. **13,** 12 (1964).
[18]T. Shinoda, H. Chihara, and S. Seki, J. Phys. Soc. Jap. **19,** 1637 (1964).
[19]A. Herweijer, W. J. M deJonge, A. C. Botterman, A. L. M. Bongaarts, and J. A. Cowen, Phys. Rev. B **5,** 4618 (1972).